 CMC, vol.12, no.3, pp.223-235, 2009

Computer Modeling of Ionic Conductivity in Low Temperature Doped Ceria Solid Electrolytes

Shu-Feng Lee[1] **and Che-Wun Hong**[1,2]

Abstract: Solid oxides, such as ceria (CeO_2) doped with cations of lower valance, are potential electrolytes for future solid oxide fuel cells. This is due to the theoretically high ionic conductivity at low operation temperature. This paper investigates the feasibility of two potential electrolytes which are samarium-doped ceria (SDC) and gadolinium-doped ceria (GDC) to replace the traditional yttria-stablized zirconia (YSZ). Molecular simulation techniques were employed to study the influence of different dopant concentrations at different operation temperatures on the ionic conductivity from the atomistic perspective. Simulation results show that the optimized ionic conductivity occurs at 11.11mol% concentration using both dopants of Gd_2O_3 and Sm_2O_3. The temperature effect was also examined under a fixed concentration simulation to check how low temperature they still function. The predicted ionic conductivities have been verified with published experimental results and show reasonable agreements. This simulation technique reveals a clear picture with qualitative and quantitative connection between the choice of the dopant and the improvement of the ionic conductivity of fuel cell electrolytes.

Keywords: solid oxide fuel cell, molecular dynamics, ionic conductivity

1 Introduction

Solid oxide fuel cells (SOFCs) are a promising candidate for future clean and efficient power sources ranging from portable to stationary power plants. It is because of the major merit of low price material without precious metal catalysts and great tolerance of fuel impurities. The current research topic is to develop an electrolyte with higher ionic conductivity at lower operation temperature, compared to the commercially available yttria-stablized zirconia (YSZ), to enhance the performance. The ionic conductivity of the YSZ decreases dramatically when the opera-

[1] Department of Power Mechanical Engineering, National Tsing Hua University, Hsinchu 30013, Taiwan.

[2] cwhong@pme.nthu.edu.tw (corresponding author)

tion temperature is below 1073K [Singhal, Kendall (2003)]. Among many potential ceramic oxides for SOFCs, the samarium-doped ceria (SDC) and gadolinium-doped ceria (GDC) were reported to be effective at intermediate temperature operation range. Most of the researches about these new materials were based on experimental methods [Tianshu, Hing, Huang, Kilner (2002); Peng, Zhang, Cheng, Cheng, Meng (2002)]. The bulk conductivity of SDC was found to be higher than GDC when the temperature is below 500^oC [Perez-Coll, Nunez, Frade, Abrantes (2003)]. The physical and chemical properties of pure and doped ceria were studied by Mogensen, Sammes, Tompsett (2000) and they found that the properties were determined during the fabrication process. Most of the above researchers employed the AC impedance spectroscopy to measure the ionic conductivity of the ceria-based materials [Barsoukov, Macdonald (2005); Balazs, Glass (1995)]. Among these substitutive ceria ceramics, the SDC and GDC electrolytes were reported to be remarkably more excellent than the others at the intermediate temperature region [Yamashita, Ramanujachary, Greenblatt (1995)]. The experimental results indicated that the conductivity of the SDC (2.8×10^{-6}S/cm) is two orders of magnitude superior to the YSZ (6.8×10^{-8}S/cm) at 200^oC.

Although fabrication and experimental techniques were able to carry out the conductivity improvement investigation in macro scope, the ionic conduction takes place at nano-scale environment. To further understand the mechanism of the ion transport, molecular dynamics (MD) simulation is an appropriate approach to perform this task [Leach (2001)]. Shen and Atluri presented a review of the computational nanomechanics, from the methods to classical molecular dynamics simulations, and multi- temporal and spatial scale simulations [Shen and Atluri (2004)]. It is proved useful and versatile especially for nanostructure properties in solid mechanics and in transport phenomena. Examples are given such as the size effect and deformation of Ni thin films [Nair, Farkas, Kriz1 (2008)] and the nanostructure effect on carbon nanotubes [Namilae, Chandra, Srinivasan, Chandra (2007); Ghanbari, Naghdabadi (2009); Chakrabarty, Cagin (2008); Xie, Han, Long (2007)], as well as the ionic conduction mechanism in the YSZ [Yamamura, Kawasaki, Sakai (1999); Tojo, Kawaji, Atake (1999); Perumal, Sridhar, Murthy, Easwarakumar, Ramasamy (2002)]. The electrical and mechanical properties of porous electrodes in SOFC have been calculated with the multiscale model developed by Li et al [Li, Saheli, Khaleel, Garmestani (2006)].This paper is an extension of a series of research on the improvement of the ionic conductivity in various modern SOFC electrolytes using the molecular dynamics technique [Cheng, Chang, Hong (2005); Cheng, Lee, Hong (2007); Lee, Cheng, Chen, Hong (2007)]. The SDC and GDC are the major concerns and the optimal composition of the trivalent dopants will be predicted instead of the trial-and-error method using experimental techniques.

2 Mathematical Models

The basic principle of the doped ceria as an electrolyte is that the substitution of Ce^{4+} by lower valance cations, such as $Sm^{3+}$and Gd^{3+}, results in an extra charge of +1. In order to maintain the electrical neutrality, every two substitutions will form an oxygen vacancy, hence the amount of vacancies equals to half amount of the trivalent ions. The microscopic simulation system can be defined as a cubic box consists of 5x5x5 crystallographic unit cell in a face-centered-cubic (FCC) structure format, as seen in Fig.1. The Ce^{4+} ions were assigned to the positions according to the fluorite lattice arrangement; some of the ions were randomly substituted by Sm^{3+} (or Gd^{3+}) ions. The oxygen ions were assigned to the center surrounded by the Ce tetrahedron; and some of them were randomly substituted by oxygen vacancies. The total number of atoms is 1500, which includes 1000 anions and 500 cations. This paper considers with four different concentrations of Sm_2O_3(or Gd_2O_3) which are 5.26 mol%, 11.11 mol%, 17.64 mol% and 25.0 mol% respectively. The amount of each atom is an integer and varies with the concentration of the dopants. Table 1 shows the simulation cases, in which case 1 to case 4 are different concentrations at a fixed temperature (873K), and case 5 to case 8 are different operation temperatures at a fixed concentration (11.11 mol%).

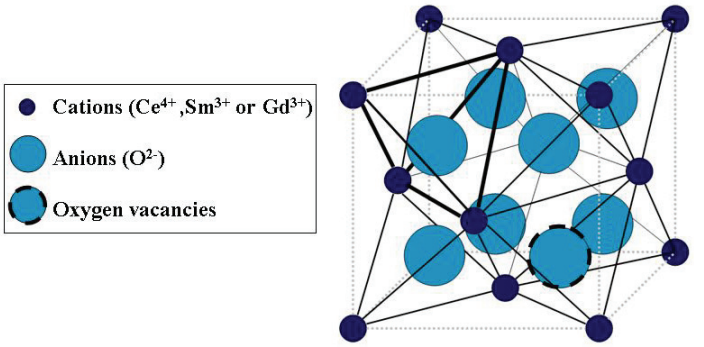

Figure 1: Schematic diagram of the initial doped ceria structure. The Ce^{4+} ions were assigned to the positions according to the FCC lattice; some of the ions were randomly substituted by Sm^{3+} (or Gd^{3+}) ions. The oxygen ions were assigned to the center surrounded by the Ce tetrahedron; and some of them were randomly substituted by vacancies.

A pair potential function called Born-Meyer-Buckingham equation was adopted to represent the short range interaction between atoms. The interaction potential

Table 1: Amount of atoms under different simulation cases for the SDC (and GDC)

Case	Sm_2O_3 (Gd_2O_3) (mol%)	Temperature (K)	Ce	Sm (or Gd)	O	Vacancies
Case 1	5.26	873	450	50	975	25
Case 2	11.11	873	400	100	950	50
Case 3	17.64	873	350	150	925	75
Case 4	25.0	873	300	200	900	100
Case 5	11.11	1073	400	100	950	50
Case 6	11.11	973	400	100	950	50
Case 7	11.11	773	400	100	950	50
Case 8	11.11	673	400	100	950	50

function is expressed by:

$$u(r_{ij}) = -\frac{A_{ij}}{r_{ij}^6} + C_{ij}\exp(-r_{ij}/\rho_{ij}) + u_{Coulombic} \tag{1}$$

wherer_{ij} is the distance between two atoms; A_{ij}, C_{ij} and ρ_{ij} are empirical constants as listed in Table 2 [Lewis, Catlow (1985)]; $u_{Coulombic}$ denotes the Coulombic potential which is induced by the charged ions. The first term at the right hand side represents the attractive effect between atoms; the second term is due to the repulsive force. Both terms only account for the short range potential. The interaction between atoms exceeding the cutoff radius, set to be 8 Å, was neglected to increase the computation efficiency. The charges of Ce, Sm (or Gd) and O were set as +4, +3 and -2 respectively. The periodic boundary conditions were applied to all directions and the simulation was carried out under NVT (fixed number of atoms, volume and temperature) ensemble using the 5^{th} order Gear's predictor-corrector algorithm [Gear (1971)] with time step of 1 fs. The long-range electrostatic interation in the Coulombic term was solved by the Ewald summation technique [Allen, Tildesley (1987)]. The volume of the unit cell varies with temperature by considering the thermal expansion effect. The side length of the simulation system follows the relation as below [Yokokawa, Horita, Sakai, Dokiya, Kawada (1996)]:

$$L(T) = L_0[1 + \alpha(T - 300)] \tag{2}$$

where L is the system length and L_0 *(at T=298K)*=5.4036 Å. The thermal expansion coefficients α=$1.1\times10^{-5}\mathrm{K}^{-1}$. All parameters used in the simulation are summarized in Table 2 as below.

Table 2: Potential coefficients between the ion-pairs in the molecular simulation

Ion pair	A_{ij}[kJ/mol]	$\rho_{ij}[\dot{A}]$	C_{ij}[kJ$\dot{A}^6$/mol]
Ce-Ce	0	1	0
Ce-Sm	0	1	0
Ce-Gd	0	1	0
Sm-Sm	0	1	0
Gd-Gd	0	1	0
Ce-O	$1.745*10^5$	0.3547	1967
Sm-O	$1.875*10^5$	0.3414	2072
Gd-O	$1.818*10^5$	0.3399	1961
O-O	$9.209*10^5$	0.2192	3086

3 Results and Discussion

A self-written soft sphere MD program was performed to carry out the simulation of the oxygen ion transport inside the solid electrolyte. The simulation procedure can be divided into two stages which are the equilibration stage and the production stage [Haile (1997)]. The durations of the equilibration and the production stages were set to be 100 ps and 500 ps respectively. The mobility of the oxygen ions can be determined by means of evaluation of the mean square displacement (MSD), which is the summation of the square of the variation of each atom position at each instant. The diffusion coefficient D can also be evaluated from the following equation:

$$MSD(t) = \frac{1}{N}\sum_{n=1}^{N}\left\langle[\overrightarrow{r_n}(t_0+t) - \overrightarrow{r_n}(t_0)]^2\right\rangle = B + 6D(t) \tag{3}$$

where N is the number of total atoms;$r_n$denotes the position vector; the brackets$\langle\rangle$ represents the time average from t_0 to t_0+t; B is a constant, and $D(t)$ is the diffusion coefficient of atoms or ions. The oxygen ion conductivity can then be determined from the diffusion coefficient using the Nernst-Einstein relation as below:

$$\sigma = \frac{Nq^2 D_{tracer}}{k_B T H_R} \tag{4}$$

where σ is the ionic conductivity; N is the number density of oxygen ions; q is the electric charge; D_{tracer} is the traced diffusion coefficient which is evaluated from the slope of the MSD versus elapsed time diagram; k_B is the Boltzmann constant; T is the system temperature; and H_R is the Haven coefficient, which was set to be one.

Simulations of different doping concentrations were then performed for the two different solid electrolytes (SDC and GDC) respectively. The MSD of the oxygen ion versus elapsed time diagrams under different doping concentrations are shown in Fig. 2. The fluctuated MSD results are smoothed by curve fitting with linear functions to indicate the diffusion coefficient. Although higher doping concentrations may produce more vacancies and help oxygen ions hop more frequently, the plot reveals that doping more Sm^{3+}(or Gd^{3+}) to Ce^{4+} will not necessarily result in higher diffusion coefficients and neither ionic conductivities. This is due to the fact that more trivalent ions will also increase forces from other cations, that makes oxygen ions stay around Ce^{4+} and vacancies appear near the Sm^{3+} (or Gd^{3+}). This phenomenon can be explained from Fig. 3; in which the radial distribution function (RDF), denoted by $g(r)$, is defined by

$$g(r) = \frac{2\langle N(r,\Delta r)\rangle}{N\rho V(r,\Delta r)} \tag{5}$$

where $N(r,r)$ is the number of atoms within a spherical shell of radius$r$+r; N is the total number of atoms in the system; ρ is the number density; $V(r,r)$ is the volume of the shell and $\langle\rangle$ indicates time average. The RDF is used to study the local ion distribution in the molecular structure. In Fig. 3(a), the amount of Ce–O, Sm-O and Gd–O ion pairs are compared at different radius and indicate that most oxygen ions stay around the Ce^{4+}. While in Fig. 3(b), the oxygen vacancies tend to stay around the Sm^{3+} and Gd^{3+} sites. The competition between the increased mobility due to increased vacancies and the decreased mobility due to increased attractive forces will result in an optimal concentration of the dopants. Figure 4 shows that the ionic conductivity in the simulation case 2 is the highest among four cases of different concentrations at the same temperature 873 K. The optimum appears at the concentration of 11.11 mol% Sm_2O_3 and the same result for the case of Gd_2O_3. The simulation results are also compared with experimental data reported by Tianshu et al (2002) and Peng et al (2002) in the diagram. Although the ionic conductivity predictions are not so exactly correct, the trends of the conductivity variation versus the concentration are exactly predicted. The magnitudes of predictions are always greater than the experimental results. This is due to the fact that the defects and grain boundaries in the molecular structure during the molecular dynamics simulation are not considered. Also the discrepancy between the idealized nano-scale simulation and the macro-scale experiment exists inherently.

The thermal effect on the ionic conductivity in the new solid electrolytes is also studied in this paper. This is to investigate how low temperature the electrolytes can still function. The low temperature operation is mainly for the concern of rapid startup and thermal durability in engineering applications. Figure 5 shows the MSDs of oxygen ions versus elapsed time at different operation temperatures.

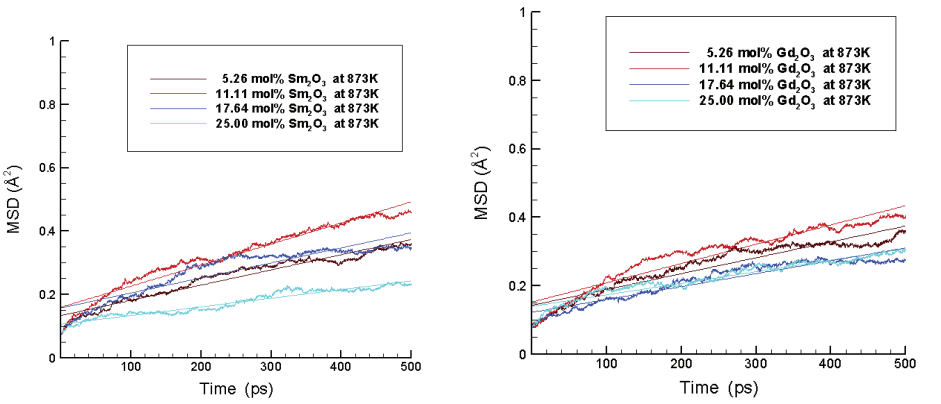

(a) SDC (b) GDC

Figure 2: Mean square displacements (MSDs) of oxygen ions for various concentrations (5.26 mol%, 11.11 mol%, 17.64 mol% and 25.00 mol% respectively) at the operation temperature 873K for (a) SDC (b) GDC. The fluctuated MSD results are smoothed by curve fitting with linear functions to indicate the diffusion coefficient.

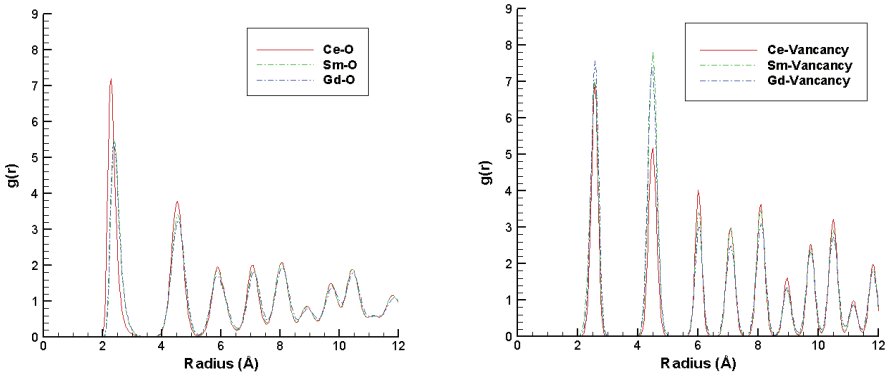

(a) (b)

Figure 3: (a) Radial distribution function $g(r)$ of Ce-O, Sm-O and Gd-O; (b) $g(r)$ of Ce-vancancy, Sm-vancancy and Gd-vancancy ion pairs for 11.11 mol% concentration at 873K.

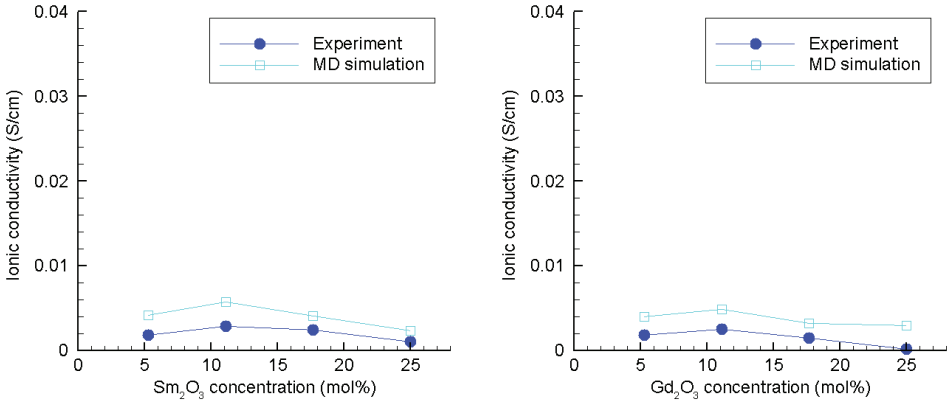

(a) SDC (b) GDC

Figure 4: Comparison of predictions and experimental data, case (a) from Peng et al (2002) and case (b) from Tianshu et al (2002), of the oxygen ionic conductivities for various concentrations (5.26 mol%, 11.11 mol%, 17.64 mol% and 25.00 mol%) at 873K.

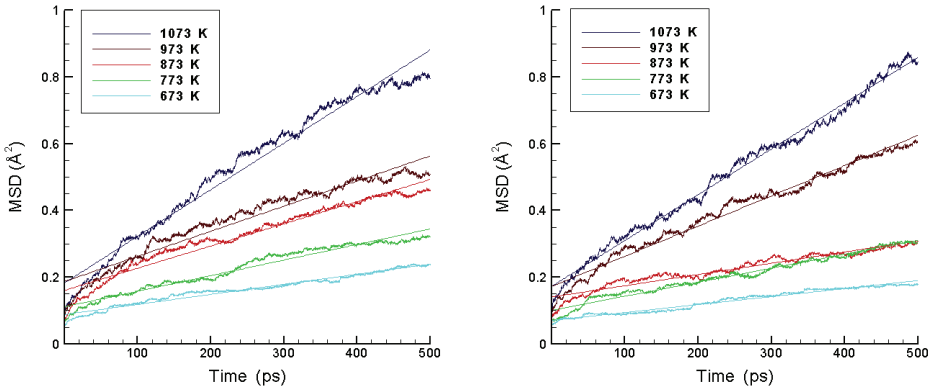

(a) SDC (b) GDC

Figure 5: Mean square displacements of oxygen ions at different operation temperatures (673K, 773K, 873K, 973K and 1073K) at the concentration 11.11 mol% of (a) SDC and (b) GDC. The higher the operation temperature, the greater the ionic mobility.

Similar to the previous cases, the MSDs are approximated by a linear function and it shows that increasing temperature enhances the diffusion of oxygen ions. Increases in mobility of oxygen ions are caused by the higher kinetic energy provided by the higher temperature operation. The tendency indicates that the higher the temperature, the larger the ionic conductivity in any cases. Figure 6 shows the comparison of predictions and experimental data. The same variation trend is also obtained and the predictions are higher than the experiments. The lowest operation temperature in both SDC and GDC goes to 673K, which is impossible for the current commercially available YSZ electrolytes.

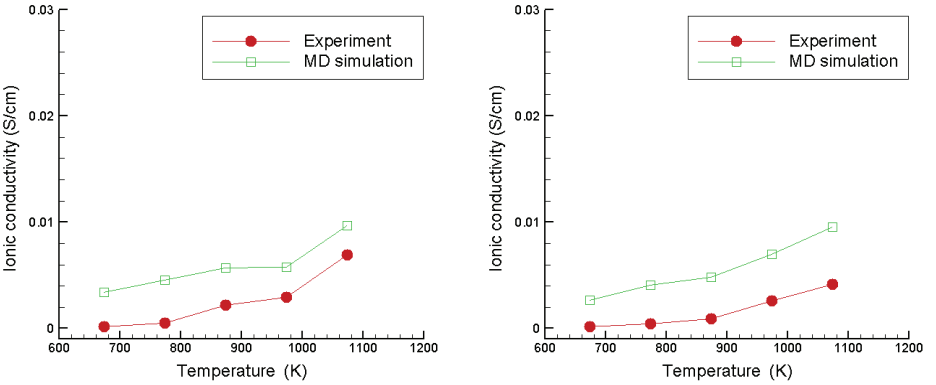

(a) SDC (b) GDC

Figure 6: Comparison of predictions and experimental data, case (a) from Peng et al (2002) and case (b) from Tianshu et al (2002), of the ionic conductivities for different temperatures (673K, 773K, 873K, 973K and 1073K). Note that the lowest operation temperature goes to 673K.

The significant dependence of the ionic conductivity on the temperature and the chemical activation energy can be examined by the log form of the Arrhenius law as below:

$$\ln(\sigma \cdot T) = \ln(A) - \frac{E_a}{k_B}(\frac{1}{T}) \tag{6}$$

where A is the pre-exponential factor; E_a is the activation energy. In this paper we examine the operation range between 673K and 1073K. The relation between $\ln(\sigma T)$ and the reciprocal temperature $(1/T)$ can be plotted as an Arrhenius diagram as shown in Fig. 7. Since the Arrhenius plots for SDC and GDC show linear tendency, the activation energy and the pre-exponential factor can both be determined.

The value of the extrapolated "y-intercept" corresponds to ln(A), and the gradient of the straight line equals to $(-E_a/k_B)$. Figure 7 shows that the influence of temperature on the ion diffusion rate is under a thermally activated process. The activation energies are evaluated from the slopes in the diagram and they are 0.216eV and 0.261eV for SDC and GDC respectively.

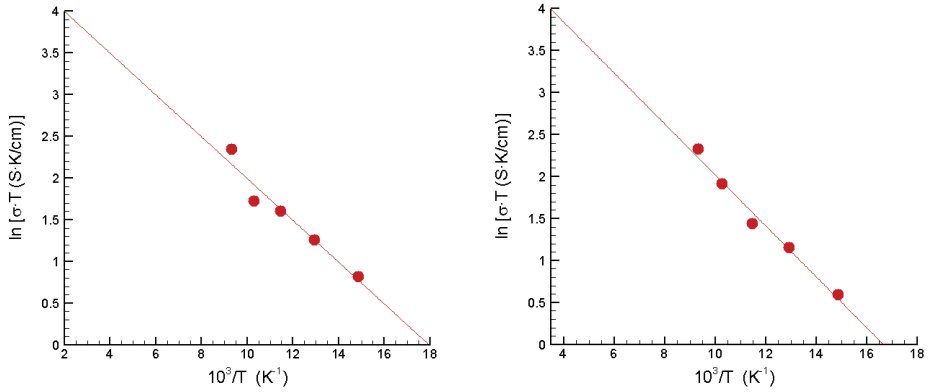

(a) SDC (b) GDC

Figure 7: Arrhenius plots of the ionic conductivity versus the reciprocal temperature for (a) SDC and (b) GDC.

4 Conclusions

Computer modeling of ionic conductivity in solid electrolytes is essentially important for developing future high-performance low-temperature operation solid oxide fuel cells. An atomistic scale simulator for ionic conductivity prediction has been set up by employing the molecular dynamics techniques. SDC and GDC were proven to be effective at intermediate and low temperature operation regions for the future SOFCs. Optimal dopant concentrations for the SDC and GDC or any other kind of new electrolytes can be predicted before fabrications. The thermal effect was also studied under a fixed concentration simulation. Results show that the operation temperature is able to lower down to 673K for both SDC and GDC. This enhances the low temperature rapid startup ability and greater thermal durability for the high temperature fuel cells. Although the simulation results are not exactly same as the experimental data, the discrepancy is within reasonable tolerance and the variation tendency is well predicted using our simulator. The simulation information provided by this work is important in developing lower temperature SOFC

electrolytes. The SDC and GDC are proven to be excellent candidates.

Acknowledgement: This research was supported by the National Science Council (Taiwan) under contracts of NSC 96-2221-E-007-061 and NSC 97-ET-7-007-007-ET. Financial supports to Mr. S.F. Lee are gratefully appreciated. We are also grateful to the National Center for High-performance Computing for providing computing facilities.

References

Allen, M. P.; Tildesley, D. J. (1987): *Computer Simulation of Liquids: Some Tricks of The Trade*, pp.156, Oxford, Clarendon.

Balazs, G. B.; Glass, R. S. (1995): AC impedance studies of rare earth oxide doped ceria, *Solid State Ionics*, vol. 76, pp. 155-162.

Barsoukov, E.; Macdonald, J. R. (2005): *Impedance Spectroscopy Theory, Experiment, and Applications*, 2^{nd} Edition, John Wileys & Sons.

Chakrabarty, A.; Cagin, T. (2008): Computational studies on mechanical and thermal properties of carbon nanotubes based nanostructures, *CMC: Computers, Materials, & Continua*, vol. 7(3), pp.167-189.

Cheng, C. H.; Chang, Y. W.; Hong, C. W. (2005): Multi-scale parametric studies on the transport phenomenon of a solid oxide fuel cell, *Journal of Fuel Cell Science and Technology*, vol. 2, pp. 219-225.

Cheng, C. H.; Lee, S. F.; Hong, C. W. (2007): Ionic dynamics of an intermediate-temperature yttria-doped-ceria electrolyte, *J. of The Electrochemical Society*, vol. 154, E158-163.

Gear, C. W. (1971): *Numerical Initial Value Problems in Ordinary Differential Equations: Chapter 9*, Englewood Cliffs, NJ.

Ghanbari, J. ; Naghdabadi, R. (2009): Multiscale nonlinear constitutive modeling of carbon nanostructures based on interatomic potentials, *CMC: Computers, Materials, & Continua*, vol. 10(1), pp.41-64.

Haile, J. M. (1997): *Molecular Dynamics Simulation: Elementary Methods*, Wiley Press, New York,USA.

Leach, A. R. (2003): *Molecular Modelling Principles and Applications*, 2^{nd} Edition, Prentice Hall.

Lee, S. F.; Cheng, C. H.; Chen, W. H.; Hong, C. W. (2007): Nano-scale analysis of low temperature solid oxide fuel cell electrolytes, *ECS Transactions-Solid Oxide Fuel Cells*, vol. 7(1), pp. 2253-2260.

Lewis, G. V.; Catlow, C. R. A. (1985): Potential models for ionic oxides, *Journal*

of Physics C: Solid State Physics, vol. 18, pp.1149-1161.

Li, D.; Saheli, G.; Khaleel, M.; Garmestani, H. (2006): Microstructure optimization in fuel cell electrodes using materials design, *CMC: Computers, Materials, & Continua*, vol. 4, pp. 31-42.

Mogensen, M.; Sammes, N. M.; Tompsett, G. A. (2000): Physical, chemical and electrochemical properties of pure and doped ceria, *Solid State Ionics*, vol. 129, pp. 63-94.

Nair, A. K.; Farkas, D.; Kriz1, R. D. (2008): Molecular dynamics study of size effects and deformation of thin films due to nanoindentation, *CMES: Computer Modeling in Engineering & Sciences*, vol. 24(3), pp. 239-248.

Namilae, S.; Chandra, U.; Srinivasan, A.; Chandra, N. (2007): Effect of interface modification on the mechanical behavior of carbon nanotube reinforced composites using parallel molecular dynamics, *CMES: Computer Modeling in Engineering & Sciences*, vol. 22(3), pp.189-202.

Peng, C.; Zhang, Y.; Cheng, Z. W.; Cheng, X.; Meng, J. (2002): Nitrate–citrate combustion synthesis and properties of $Ce_{1-x}Sm_xO_{2-x/2}$ solid solutions, *Journal of Materials Science: Materials in Electronics*, vol. 13, pp.757-762.

Perez-Coll, D.; Nunez, P.; Frade, J. R.; Abrantes, J. C. C. (2003): Conductivity of CGO and CSO ceramics obtained from freeze-dried precursors, *Electrochimica Acta*, vol. 48, pp.1551-1557.

Perumal, T. P.; Sridhar, V.; Murthy, K. P. N.; Easwarakumar, K. S.; Ramasamy, S. (2002): Molecular dynamics simulations of oxygen ion diffusion in yttria-stabilized zirconia, *Physica A*, vol. 309(1-2), pp. 35-44.

Singhal, S. C.; Kendall, K. (2003): *High Temperature SOFCs: Fundamentals, Design and Applications*, Elsevier.

Shen, S.; Atluri, S.N. (2004): Computational nano-mechanics and multi-scale simulation, *CMC: Computers, Materials, & Continua*, vol. 1, pp. 59-90.

Tianshu, Z.; Hing P.; Huang H.; Kilner J. (2002): Ionic conductivity in the CeO_2–Gd_2O_3 system ($0.05 \leq Gd/Ce \leq 0.4$) prepared by oxalate coprecipitation, *Solid State Ionics*, vol. 148, pp. 567-573.

Tojo, T.; Kawaji, H.; Atake, T. (1999): Molecular dynamics study on lattice vibration and heat capacity of yttria-stabilized zirconia, *Solid State Ionics*, vol. 118(3-4), pp. 349-353.

Xie, G.Q.; Han, X.; Long, S.Y. (2007): Characteristic of waves in a multi-walled carbon nanotube, *CMC: Computers, Materials, & Continua*, vol. 6(1), pp.1-11.

Yamamura, Y.; Kawasaki, S.; Sakai, H. (1999): Molecular dynamics analysis of ionic conduction mechanism in yttria-stabilized zirconia, *Solid State Ionics*, vol.

126(1), pp. 181-189.

Yamashita, K.; Ramanujachary, K. V.; Greenblatt, M. (1995): Hydrothermal synthesis and low temperature conduction properties of substituted ceria ceramics, *Solid State Ionics*, vol. 81, pp. 53-60.

Yokokawa, H.; Horita, T.; Sakai, N.; Dokiya, M.; Kawada, T. (1996): Thermodynamic representation of nonstoichiometric lanthanum manganite, *Solid State Ionics*, vol. 86-88, pp. 1161-1165.